

# Characterization of Plaque Components With Intravascular Ultrasound Elastography in Human Femoral and Coronary Arteries In Vitro

Chris L. de Korte, PhD; Gerard Pasterkamp, PhD, MD; Anton F.W. van der Steen, PhD;  
Hein A. Woutman, MSc; Nicolaas Bom, PhD

**Background**—The composition of plaque is a major determinant of coronary-related clinical syndromes. Intravascular ultrasound (IVUS) elastography has proven to be a technique capable of reflecting the mechanical properties of phantom material and the femoral arterial wall. The aim of this study was to investigate the capability of intravascular elastography to characterize different plaque components.

**Methods and Results**—Diseased human femoral (n=9) and coronary (n=4) arteries were studied in vitro. At each location (n=45), 2 IVUS images were acquired at different intraluminal pressures (80 and 100 mm Hg). With the use of cross-correlation analysis on the high-frequency (radiofrequency) ultrasound signal, the local strain in the tissue was determined. The strain was color-coded and plotted as an additional image to the IVUS echogram. The visualized segments were stained on the presence of collagen, smooth muscle cells, and macrophages. Matching of elastographic data and histology were performed with the use of the IVUS echogram. The cross sections were segmented in regions (n=125) that were based on the strain value on the elastogram. The dominant plaque types in these regions (fibrous, fibro-fatty, or fatty) were obtained from histology and correlated with the average strain and echo intensity. The strain for the 3 plaque types as determined by histology differed significantly ( $P=0.0002$ ). This difference was mainly evident between fibrous and fatty tissue ( $P=0.0004$ ). The plaque types did not reveal echo-intensity differences in the IVUS echogram ( $P=0.882$ ).

**Conclusions**—Different strain values are found between fibrous, fibro-fatty, and fatty plaque components, indicating the potential of intravascular elastography to distinguish different plaque morphologies. (*Circulation*. 2000;102:617-623.)

**Key Words:** atherosclerosis ■ elasticity ■ plaque ■ ultrasonics ■ catheters

Intravascular ultrasound (IVUS) currently is the only clinically available technique providing real-time cross-sectional images of the vascular wall. Although IVUS imaging reveals the geometry of the vessel wall and plaque, characterization of the plaque composition remains difficult. Calcified and fibrous plaques can be identified in most of the cases.<sup>1-4</sup> Calcified areas are identified by their hyperechoic appearance and distal shadowing and may be associated with acoustic reverberation. Fibrous lesions yield homogeneous echo reflections without distal shadowing. However, the composition of lipid-containing and mixed (fibrous, lipid-calcified) plaques remains unknown in most of the cases.<sup>1,2,5</sup> Knowledge about plaque composition can assist the clinicians in choosing the proper interventional technique. Moreover, since most interventional techniques are predominantly mechanical in nature,<sup>6</sup> the outcome of the intervention may be influenced by the mechanical properties of the vessel wall and plaque.<sup>7</sup>

The composition of plaque is a major determinant of clinical syndromes.<sup>8,9</sup> Additionally, vulnerability of plaque is influenced by the mechanical properties of the vessel wall and plaque. Studies revealed that a thin cap overlying fatty tissue may be unable to bear the imposed stress caused by the pulsatile pressure of the blood.<sup>10,11</sup> Lipid-rich lesions with a thin cap and local inflammatory response are considered rupture prone, which may lead to subsequent thrombosis and myocardial ischemia. Therefore, techniques that are capable of characterizing the plaque may bear clinically relevant diagnostic, prognostic, and etiological values.<sup>12</sup> In IVUS imaging, the mechanical properties of the atherosclerotic plaque is not necessarily related to its echogenicity.<sup>7</sup>

Intravascular elastography is a new technique based on IVUS. The technique is in principle able to discriminate between soft and hard material. The underlying principle is that soft material will strain more compared with hard material when a force is applied on the tissue.<sup>13</sup> The strain is

Received October 18, 1999; revision received February 21, 2000; accepted February 29, 2000.

From Experimental Echocardiography, Thoraxcentre, Rotterdam, The Netherlands (C.L.d.K., A.F.W.v.d.S., N.B.); University Hospital, Utrecht, The Netherlands (G.P., H.A.W.); and Interuniversity Cardiology Institute of the Netherlands, Utrecht (G.P., A.F.W.v.d.S., N.B.).

Correspondence to Chris L. de Korte, Experimental Echocardiography, Ee23.02, Erasmus University Rotterdam, Dr Molewaterplein 50, PO Box 1738, 3000DR Rotterdam, The Netherlands. E-mail dekorte@tch.fgg.eur.nl

© 2000 American Heart Association, Inc.

*Circulation* is available at <http://www.circulationaha.org>

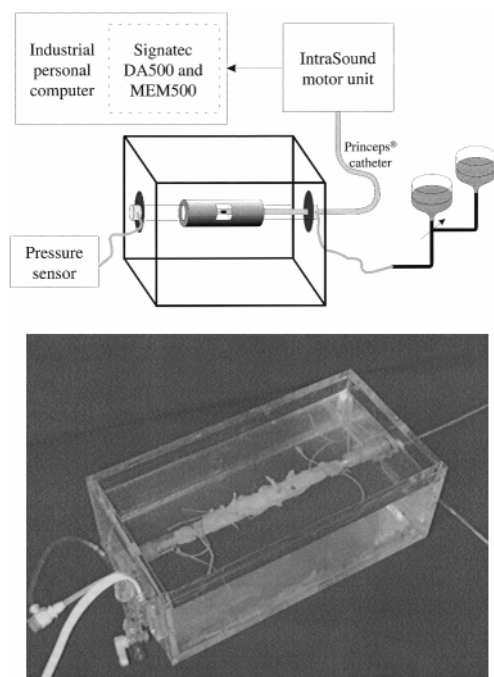


**Figure 1.** Top, Experimental setup with water tank, water column system, pressure sensor, catheter connected to motor unit, and data acquisition system. Bottom, Photograph of water tank with diseased human femoral artery. Side branches are all closed with suture.

determined by means of the ultrasound signal. The method was validated and applied *in vivo* for tumor detection in breast.<sup>14</sup> Currently, this technique is being developed for intravascular purposes<sup>15–17</sup> and applied on human arteries *in vitro*<sup>18</sup>: Preliminary experiments revealed that it is feasible to identify different tissue components with the use of intravascular elastography. Since the images are based on the radial strain, the technique has potentials to detect regions with elevated stress: An increased circumferential stress will result in an increased radial strain of the material.

The aim of the present study was to investigate the capability of intravascular elastography to differentiate between different plaque components. We hypothesized that fibrous, fibro-fatty, and fatty tissue could be discriminated by means of the elastogram. Intravascular elastograms were obtained of diseased human femoral and coronary arteries *in vitro*. After the ultrasound experiments, the arteries were processed for histological analysis. Regions with different elastographic values were correlated with the predominant plaque morphology as determined histologically.

## Methods

### Materials

Atherosclerotic human femoral ( $n=10$ ) and coronary ( $n=4$ ) artery segments were excised within 24 hours after death and stored at  $-70^{\circ}\text{C}$ . The arteries were thawed at  $4^{\circ}\text{C}$  and connected to both the insertion sheaths of the experimental setup (Figure 1) and tied with suture material after closing side branches with suture material. Since the *in vivo* length of the specimens was unknown, the arteries were not stretched along the vessel axis. One femoral artery was excluded because the acquisition of radiofrequency data failed during this experiment. The arteries were scanned at different positions, with an interspacing of  $\geq 10$  mm. These cross sections

( $n=65$ ) were marked with a surgical needle, inserted in the periventricular, which is clearly visible in the echogram. After the ultrasound experiment, a suture was used to connect a marker to the outside of the vessel wall at the position of the needle.

### IVUS Experiments

The ultrasound experiments were performed in a physiological saline solution in a water tank at room temperature ( $21 \pm 2^{\circ}\text{C}$ ).<sup>18</sup> A water column system, containing a degassed physiological saline solution, was connected to the proximal sheath. Intraluminal pressures of 80 and 100 mm Hg were applied. This sheath also was used to insert the echo catheter. The femoral and coronary arteries were scanned with a Priniceps 30-MHz IVUS catheter and an InVision 20-MHz IVUS catheter, respectively (both EndoSonics). The pressure was monitored with the use of a pressure gauge (DTX/plus, Ohmeda) connected to the distal sheath.

The Priniceps catheter was connected to a modified IntraSound (EndoSonics) motor unit. This unit contains the pulser and receiver of the echographic system and a stepper motor to rotate the single-element transducer in 400 steps per revolution. At each angle, 12 traces of  $10.0\text{-}\mu\text{s}$  radiofrequency data were acquired. These 12 traces were averaged to increase the signal-to-noise ratio. The data were stored in an industrial-grade Pentium computer, equipped with a 200-MHz sampling frequency acquisition board (Signatec).

The Visions catheter was connected to an InVision echo apparatus (EndoSonics); 512 angles containing  $5\ \mu\text{s}$  of radiofrequency data sampled at 100 MHz were stored by means of a built-in procedure.

Elastograms were calculated as described by de Korte et al.<sup>18</sup> First, an IVUS frame was acquired at 80 mm Hg intravascular pressure (Figure 2a). After 2 seconds, an IVUS frame was acquired at 100 mm Hg (Figure 2b) to achieve different strain levels of the material. With the use of cross-correlation techniques, the local strain was calculated from the gated radiofrequency traces. First, the displacement of the tissue at increasing depths was determined. Next, the differential displacement of the tissue was directly converted to strain ( $\epsilon$ ). The strain values were color-coded from red for low strain through yellow to green for 1% strain (traffic-light notation) and plotted as a complementary image to the IVUS echogram (Figure 2c). The resolution of the strain in the radial direction is  $200\ \mu\text{m}$ .

### Histology

After the ultrasound experiments and subsequent formalin fixation, the marked arterial segments (0.5 cm) were dissected. The segments were decalcified in EDTA and subsequently processed for routine paraffin embedding. Sections of  $4\text{-}\mu\text{m}$  thickness were sliced near the center of the marked segment. For each segment, cross sections were stained for collagen with picro-Sirius red stain, for smooth muscle cells with anti- $\alpha$ -actin stain (clone 1a4, 8 mg/mL, Sigma), and for macrophages with anti-CD68 stain (kp1, 3 mg/mL, Dakopatts). The immunoreactivity of  $\alpha$ -actin and CD68 stain were enhanced with 10 mmol/L citrate and buffered at pH 6.0 for 15 minutes at  $100^{\circ}\text{C}$ . In addition, a streptavidin-biotin complex/horseradish technique was used. The picro-Sirius red stain was used in combination with polarized microscopy to estimate the amount of fatty tissue within the plaque.

### Matching IVUS and Histology

The alignment of the ultrasound data and histological cross sections was performed with the use of the IVUS echogram and histology. Many groups already have demonstrated the relation between IVUS echograms and histological sections, especially the geometry of the vessel wall and plaque.<sup>1,3,4</sup> From all cross sections ( $n=65$ ), only cross sections for which an exact match between histology and IVUS echogram ( $n=45$ ) could be made were taken for the statistical analysis. The matching was performed without knowledge of the elastographic results.

The cross sections were segmented into regions on the basis of the strain. Regions were selected with a similar strain value in the elastogram (see Figures 3 and 4). Regions with unreliable strain information were rejected: In these regions ( $n=8$ ), the estimated

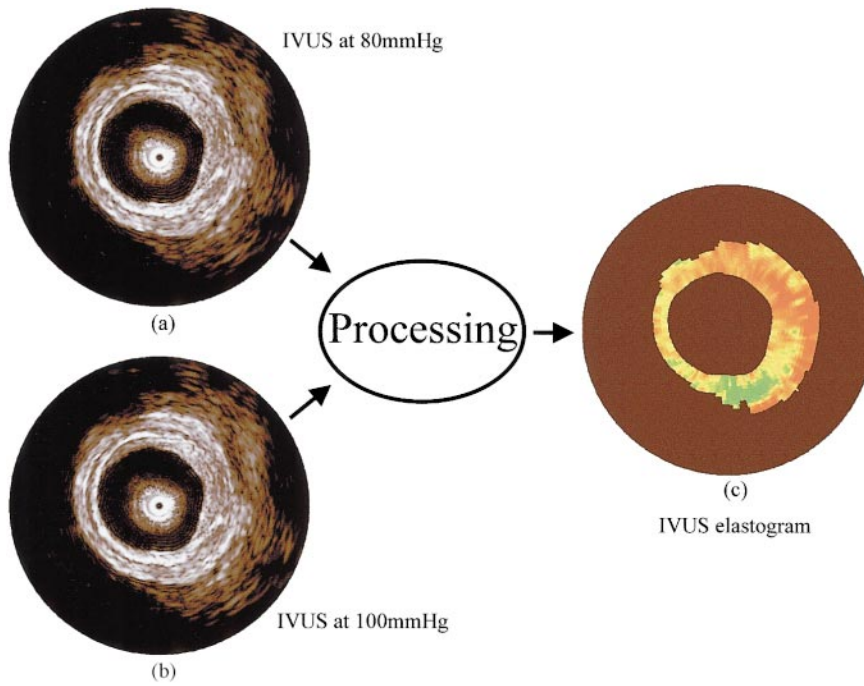


**Figure 2.** Principle of forming intravascular elastogram. IVUS echogram is acquired at intraluminal pressure of 80 mm Hg (a). Next, another IVUS echogram is acquired at 100 mm Hg intraluminal pressure (b). With cross-correlation analysis on radiofrequency signal, local strain is determined. Strain is color-coded and plotted in complementary image called intravascular elastogram (c).

strain was not in accordance with the peak value of the cross-correlation function used for the strain estimation as described previously.<sup>18,19</sup> Next, the average strain ( $\epsilon_{avg}$ ) in this region was determined. Finally, in the corresponding region in the echogram, the average echo intensity was calculated. The echo intensity is taken from the envelope that is calculated from the radiofrequency signal (digitized in 8 bits) resulting in values between 0 and 128. All data were acquired at the same gain setting. For correlation with histology, the dominant tissue types in the selected regions were determined by 2 researchers unaware of the elastographic results (H.A.W. and G.P.). The regions were subdivided into 4 tissue types: (1) fibrous tissue: >80% of the area consists of fibrous material; (2) fibro-fatty tissue: If 20% to 50% of the area was fatty material and the remaining area contained fibrous material, the dominant tissue type was fibro/fatty; (3) fatty tissue: >50% of the area consists of fatty material; and (4) vessel wall: If the echogram revealed no plaque in the region and the main content was fibrous material, the region was classified as vessel wall.

### Statistical Analysis

First, the distribution of the average strain and average echo intensity were tested for normality. All statistical analysis was performed with

the use of SAS software. These tests revealed that the strain ( $P < 0.01$ ) and the echo intensity ( $P < 0.01$ ) were not normally distributed. Next, the median and upper and lower quartiles of the average strain value and the echo intensity in the regions were determined for the 3 plaque types and vessel wall. The incremental pressure strain modulus was calculated by means of the relation  $E_{ps} = \Delta P / 2\epsilon_{avg}$ .<sup>20</sup>

After normalizing the strain and echo-intensity data by means of a square-root transformation,<sup>21</sup> a 2-way ANOVA between plaque and artery type was performed on the strain and the echo intensity, respectively. Finally, the differences between 2 plaque groups (fibrous versus fibro-fatty, fibrous versus fatty, and fibro-fatty versus fatty) were tested by means of ANOVA. Values of  $P < 0.0166$  were considered significant (Bonferroni correction).

### Results

In this study, 45 cross sections were analyzed from 13 arteries. The cross sections were segmented in regions ( $n = 125$ ). The majority of regions (Table 1) contained fibrous material (50%), the minority fatty material (10%); 27% was

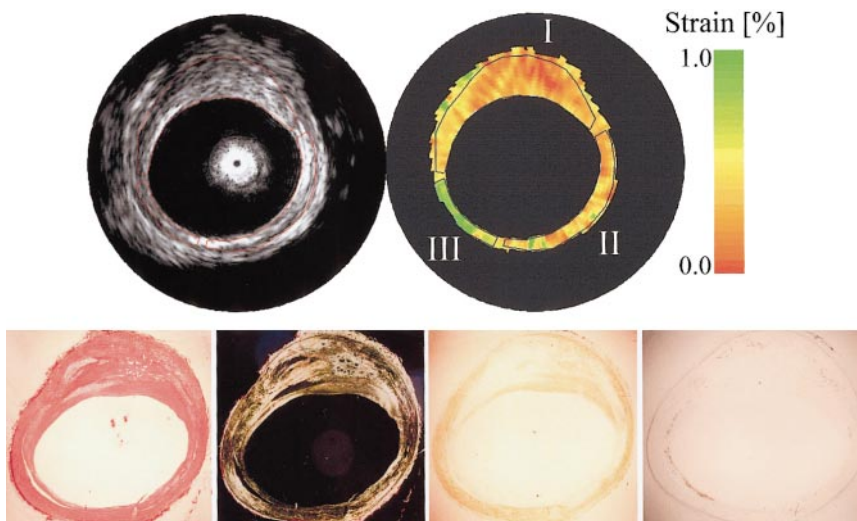


**Figure 3.** Intravascular echogram (top left) and elastogram (top right) of diseased human femoral artery with corresponding histology: (bottom row, left to right) picro-Sirius red, picro-Sirius red with polarized light microscopy, anti- $\alpha$ -actin, and anti-CD-68 antibody. Echogram reveals eccentric plaque (region I). Elastogram reveals low strain in plaque (0.24%), similar strain in non-diseased vessel wall between 3 and 7 o'clock positions (0.32%), and high strain in vessel wall between 7 and 9 o'clock positions (0.96%). Histology reveals fibrous composition of plaque (bottom row, first 2 panels on left). Region with high strain contains fatty foam cells at lumen-vessel wall boundary and increased macrophage activity (bottom row, far right).



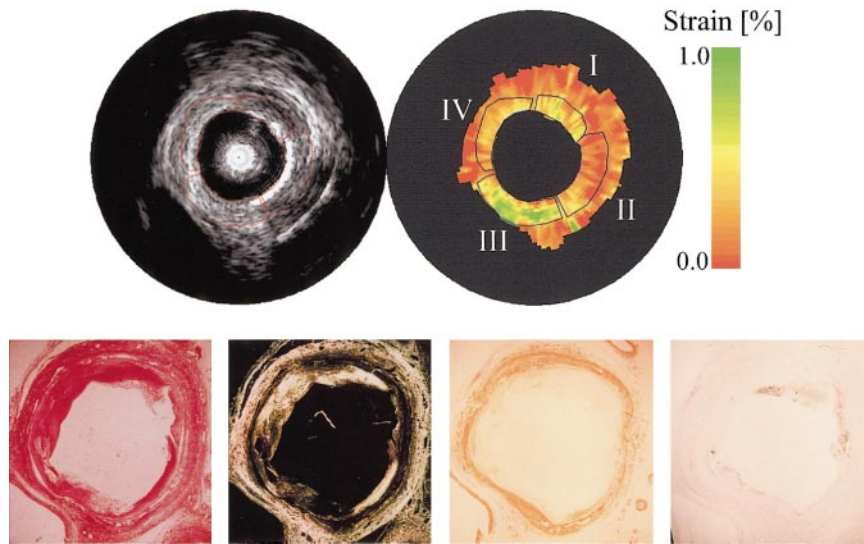


**Figure 4.** Intravascular echogram (top left) and elastogram (top right) of diseased human femoral artery with corresponding histology: (bottom row, left to right) picro-Sirius red, picro-Sirius red with polarized light microscopy, anti- $\alpha$ -actin, and anti-CD-68 antibody. Echogram shows concentric plaque with different echogenicities for regions. Elastogram reveals 2 soft regions (region I and region III) and 2 harder regions (region II and region IV). Histology reveals that 2 soft regions contain fatty material and 2 harder regions mainly contain fibrous material. Macrophage concentration is also increased in soft regions.

mixed fibro-fatty material, and 13% of the regions contained nondiseased vessel wall material.

An IVUS echogram and elastogram of a femoral artery cross section are presented in Figure 3. The echogram reveals an eccentric plaque between the 9 and 3 o'clock positions. The elastogram shows that the strain in the plaque is low. The strain in the vessel wall is similar to the strain in the plaque except for region III; increased strain values are found in this region. The histology reveals that the dominant plaque component is fibrous material. The vessel wall with increased strain values has fatty tissue components at the lumen-vessel-wall boundary, with fibrous tissue components more distally. Additionally, an increased macrophage concentration is observed in the region with high strain values. Note that the echogenicity among these regions was similar, implying that the difference in composition between this region and the remaining arterial wall could not be made with the use of the IVUS echogram.

Another example is presented in Figure 4. The IVUS echogram shows a concentric plaque with different echogenicities. The elastogram reveals 2 regions with low strain values and 2 regions with increased strain values. The histology reveals that the regions with increased strain correspond to lipid-rich regions and the regions with low strain values to fibrous plaque components. The difference between the different regions could not be observed with the use of the echogram because the echo intensity in region III and region IV is similar but the dominant tissue type is not.

**TABLE 1. Median Strain Values for the 3 Different Plaque Types and Normal Vessel Wall for All Observations and Femoral and Coronary Arteries Separately**

|                    | All Data<br>(n) | Femoral<br>(n) | Coronary<br>(n) |
|--------------------|-----------------|----------------|-----------------|
| Fibrous tissue     | 0.27 (62)       | 0.27 (48)      | 0.30 (14)       |
| Fibro-fatty tissue | 0.45 (34)       | 0.41 (25)      | 0.50 (9)        |
| Fatty tissue       | 0.60 (13)       | 0.66 (7)       | 0.57 (6)        |
| Normal vessel wall | 0.44 (16)       | 0.44 (16)      | — (—)           |
| Total regions, n   | 125             | 96             | 29              |

The box-and-whisker plot shows the median, lower, and upper quartiles and the extent of the data for the 3 plaque types and normal artery wall (Figure 5). The strain in fibrous tissue is lower than the strain in fibro-fatty tissue. Fatty tissue components are softer than fibro-fatty and fibrous tissue components. These differences are present in both femoral and coronary arteries (Table 2). The 2-way ANOVA (Table 3) shows highly significant ( $P=0.0002$ ) differences in strain among the 3 plaque types. This relation is not affected by the type of artery ( $P=0.576$ ), although significantly different strain values are observed between femoral and coronary arteries ( $P=0.019$ ). No difference in echogenicity for the 3 different plaque types was found ( $P=0.882$ ). Table 4 reveals that differences between fibrous and fatty tissue and between fibrous and fibro-fatty tissue are significant.

## Discussion

The composition and morphology of the atherosclerotic lesion rather than the degree of stenosis is currently considered an important determinant for acute coronary syn-

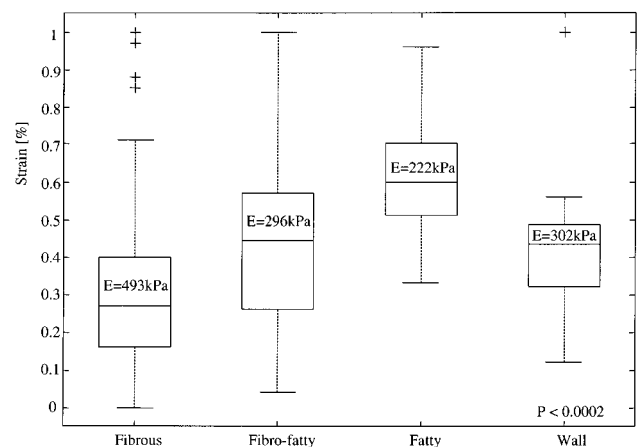


**Figure 5.** The 3 plaque types and normal vessel wall. Boxes have lines at lower, median, and upper quartile values. Whiskers show extent of remaining data. Plot reveals difference between the 3 plaque types. Highly significant difference between groups is found with 2-way ANOVA.

**TABLE 2. Median Echo Intensity Values for the 3 Different Plaque Types and Normal Vessel Wall for All Observations and Femoral and Coronary Arteries Separately**

|                    | All Data | Femoral | Coronary |
|--------------------|----------|---------|----------|
| Fibrous tissue     | 27.2     | 22.6    | 30.3     |
| Fibro-fatty tissue | 28.1     | 26.4    | 32.6     |
| Fatty tissue       | 31.4     | 23.0    | 34.2     |
| Normal vessel wall | 33.8     | 33.8    | ...      |

dromes.<sup>10–12</sup> Imaging modalities capable of characterizing the tissue of the atherosclerotic lesion may help us to understand its natural history and detect lesions with high risk for acute events.

In this study, the characterization capabilities of intravascular elastography were investigated; 125 regions were selected from 45 cross sections in 13 arteries, based on their elastographic (strain) values. After ultrasound imaging, the dominant tissue type in these regions was determined by immunostaining. The principal findings in this study were: (1) In human femoral and coronary artery specimens, the elastogram is capable of demarcating regions within the plaque representing differences in strain, whereas in the still-frame IVUS image, these regions could not be discriminated. (2) These differences in strain as observed within the elastogram were associated with differences in tissue types: lipid-rich regions revealed significantly higher strain values compared with fibrous-rich regions.

The results of this study demonstrate that characterization of different plaque components is feasible with intravascular elastography. A great advantage of this technique is that it is based on available clinical instruments. This in contrast to other imaging techniques capable of characterizing plaques such as optical coherence tomography<sup>22</sup> and Raman spectroscopy,<sup>23</sup> which still must be developed for clinical applications. The data processing now performed off-line still must be implemented in the echo apparatus. For an elastogram, only 2 IVUS echograms are required, obtained at 2 different intraluminal pressures. In vivo, different pressures are already present because of the pulsation of blood. This implies that with only a pressure sensor and an IVUS catheter, all tools for in vivo intravascular elastography are available. Thus, IVUS imaging is a technique capable of providing both qualitative as well as quantitative information on the atherosclerotic lesion.

The information in the elastogram is in principle independent of the echographic information.<sup>15,24</sup> This is an important feature, since characterization of fibrous, fibro-fatty, and fatty plaques, based on the echogram only, is limited.<sup>1,2</sup> In this

**TABLE 3. Two-Way ANOVA on Strain and Echo Intensity Between the Factors Plaque Type and Artery Type**

|                           | Strain, <i>P</i> | Echo Intensity, <i>P</i> |
|---------------------------|------------------|--------------------------|
| Plaque type               | 0.0002           | 0.8823                   |
| Artery type               | 0.0191           | 0.0013                   |
| Plaque type × artery type | 0.5758           | 0.8919                   |

**TABLE 4. Two-Way ANOVA of Strain Values Between 2 Plaque Types**

|                     | <i>P</i> |
|---------------------|----------|
| Fibrous–fibro-fatty | 0.0076   |
| Fibrous–fatty       | 0.0004   |
| Fibro-fatty–fatty   | 0.0582   |

study, no significant difference between the average echo intensity for the 3 tissue types was observed. In Figure 4, regions III and IV have a similar echo intensity, but the elastogram reveals that region IV is hard and region III is soft. The histology corroborates these elastographic findings, since region III is mainly fatty and region IV is fibrous.

The measured average strain values were converted to a pressure-strain modulus.<sup>25</sup> The pressure-strain modulus of fibrous tissue (493 kPa) is ≈2 times the pressure-strain modulus of fatty tissue (222 kPa). The pressure-strain modulus of mixed plaques has a value in between these 2 values (296 kPa). Although these values are higher than the static stiffness as measured by Lee et al,<sup>26</sup> the ratio between the modulus of the 2 groups is similar. It must be noted that the different elastic moduli are highly dependent on the different measuring techniques (static, dynamic, circumferential, tangential, and so on) and experimental methods.

### Differences Between Femoral and Coronary Arteries

This study reveals that the relation between plaque type and strain is evident irrespective ( $P=0.576$ ) of the artery type (femoral or coronary). However, different strain values for the 3 plaque types are found in femoral and coronary arteries. Especially plaques containing a large amount of fatty material have different strain values. The echo intensity in the coronary arteries is higher than in the femoral arteries for all plaque types, possibly because a different echo apparatus is used for these arteries. Again, the relation between plaque type and echo intensity is not influenced ( $P=0.892$ ) by the artery type (and thus the echo apparatus used).

### Detection of Vulnerable Plaque

The primary aim of this study was to evaluate the capability of intravascular elastography to characterize different plaque components. In patients with cardiovascular disease, plaque morphology is related to clinical presentation. Atherosclerotic plaques observed in patients with unstable angina and myocardial infarction have features associated with local thrombus formation caused by plaque rupture. The classic vulnerable plaque consists of a thin fibrous cap overlying a large atheroma with local inflammatory response beneath the surface of the cap. The present study shows that IVUS elastography is able to differentiate between lipid-rich and fibrous tissues within the plaque. In addition, a thin fibrous cap is less able to bear the circumferential stress applied on it with subsequent strain increase on the elastogram. Destruction of the collagen fibers by local inflammation may further weaken the cap and reflect additional strain increase on the elastogram. This might explain the frequently observed collocation of high strain values and macrophage-rich areas

(Figures 3 and 4). Future validation studies are necessary to investigate the effect of a thin fibrous cap and local weakening on the elastogram.

### Limitations of the Study

The elastographic experiments are performed in a water tank at room temperature. A stable intraluminal pressure was only achieved if all side branches of the arteries were perfectly closed. In some specimens, a total closure of all branches was not possible, resulting in leakage of the intraluminal saline solution and thus a pressure differential <20 mm Hg. This smaller pressure differential leads to smaller strains and increases the variance of the strain estimate for all 3 plaque types.

The elastographic measurements have been performed in a water tank at 21°C, whereas in vivo measurements are performed at 37°C. Since the mechanical properties of the tissue in the arterial wall is likely to be different at 21°C as compared with 37°C, which is particularly the case for lipid cores, this temperature drop may bring forth inaccuracy of the measurements presented. However, at temperatures >20°C, fatty tissues tend to melt,<sup>27</sup> and this will increase the difference between this tissue type and fibrous tissues.

The elastograms were matched to the histology by means of the IVUS echogram. Although the correlation between histology and IVUS echograms was already demonstrated by many studies,<sup>1,3,4</sup> matching of the IVUS and histological sections was not possible in all cases. Especially, matching of cross sections with concentric plaque with a lack of calcified areas was not reliable in some cases. In the staining process, the position of the marker was not always identifiable in the histological sections. However, exclusion of segments occurred without knowledge of the elastogram. Thus, the present observations may not be a result of selection bias.

This study was performed on excised arteries. The specimens were frozen after excision and thawed just before the ultrasound measurements. Freezing and thawing tissue has no significant influence on the acoustical properties of the tissue.<sup>28</sup> Gow and Hadfield<sup>29</sup> clearly showed that both the static and dynamic elastic moduli of arteries were elevated after excision and that further increases may occur after cold storage. However, excision of the arteries and freezing the specimens before the ultrasound experiments will affect the results when it has a different influence on the different tissue components. Since this method will be evaluated in vivo, the effect of excision and freezing can be investigated.

### Advancing Intravascular Elastography to In Vivo Applications

As already discussed, different pressure levels are normally present in the human circulatory system. In this study, the 2 echograms are acquired at 80 and 100 mm Hg. These pressures are in the range of the normal coronary pressure. With the use of time-gated data acquisition, data sets at different pressure levels can be acquired, which can be used to determine elastograms.

Especially in coronary arteries, IVUS catheters will move in the lumen because of the contraction of the heart. Not only motion in the plane of the cross sections will occur but also

motion along the long axis of the vessel. This motion along the axis of the vessel will introduce errors that are difficult to correct for because data from different parts of the artery will be acquired. However, initial measurements in human coronary arteries in vivo revealed that the motion of the catheter in the lumen is minimal near end diastole while maintaining a pressure differential large enough to strain the tissue.

### Conclusions

Intravascular elastography is a new technique that assesses the local mechanical properties of the vessel wall and plaque. The 3 plaque components fibrous, fibro-fatty, and fatty tissue result in different mean strain values. Fibrous tissue has lower strain values than fibro-fatty tissue, and the latter one has lower strain levels than fatty tissue. Identification of the 3 tissue types on the basis of the average echo intensity was not possible.

### Acknowledgments

The Dutch Technology Foundation (STW, Project RGN 44.3462) is gratefully acknowledged for financial support. The authors thank F. Mastik and J. Honkoop of the Erasmus University for their technical assistance and E.I. Céspedes from EndoSonics for his useful comments during the ultrasound experiments. H. Boersma from the Thoraxcentre is acknowledged for his advice on the statistical analysis and A. Schoneveld from the University Hospital Utrecht for his assistance in histological staining and analysis.

### References

- Potkin BN, Bartorelli AL, Gessert JM, et al. Coronary artery imaging with intravascular high-frequency ultrasound. *Circulation*. 1990;81:1575–1585.
- Yock PG, Linker DT. Intravascular ultrasound: looking below the surface of vascular disease. *Circulation*. 1990;81:1715–1718.
- Nishimura RA, Edwards WD, Warnes CA, et al. Intravascular ultrasound imaging: in vitro validation and pathologic correlation. *J Am Coll Cardiol*. 1990;16:145–154.
- Gussenhoven EJ, van der Lugt A, van der Steen AFW, et al. What have we learned from in vitro intravascular ultrasound. *Am Heart J*. 1996;132:702–710.
- Nissen SE, Ziada K, Tuczu EM. Detection of atherosclerosis and identification of vulnerable plaque: potential role of intravascular ultrasound. In: Fuster V, ed. *The Vulnerable Atherosclerotic Plaque: Understanding, Identification and Modification*. New York, NY: Futura Publishing Co Inc; 1999:87–109.
- Waller BF. Crackers, breakers, stretchers, drillers, scrapers, shavers, burners, welders and melters: the future treatment of atherosclerotic coronary artery disease. *J Am Coll Cardiol*. 1989;13:969–987.
- Hori T, Leung CY, De Guzman S, et al. Are soft echoes really soft? Intravascular ultrasound assessment of mechanical properties in human atherosclerotic tissue. *Am Heart J*. 1997;133:1–7.
- Falk E, Shah P, Fuster V. Coronary plaque disruption. *Circulation*. 1995;92:657–671.
- Fuster V, Stein B, Ambrose J, et al. Atherosclerotic plaque rupture and thrombosis: evolving concepts. *Circulation*. 1990;82(suppl II):II-47–II-59.
- Lee RT, Libby P. The unstable atheroma. *Arterioscler Thromb Vasc Biol*. 1997;17:1859–1867.
- Richardson PD, Davies MJ, Born GVR. Influence of plaque configuration and stress distribution on fissuring of coronary atherosclerotic plaques. *Lancet*. 1989;21:941–944.
- Lendon CL, Davies MJ, Born GVR, et al. Atherosclerotic plaque caps are locally weakened when macrophage density is increased. *Atherosclerosis*. 1991;87:87–90.
- Ophir J, Céspedes EI, Ponnekanti H, et al. Elastography: a method for imaging the elasticity in biological tissues. *Ultrason Imaging*. 1991;13:111–134.

14. Céspedes EI, Ophir J, Ponnekanti H, et al. Elastography: elasticity imaging using ultrasound with application to muscle and breast in vivo. *Ultrason Imaging*. 1993;17:73–88.
15. de Korte CL, Céspedes EI, van der Steen AFW, et al. Intravascular elasticity imaging using ultrasound: feasibility studies in phantoms. *Ultrasound Med Biol*. 1997;23:735–746.
16. Ryan LK, Foster FS. Ultrasonic measurement of differential displacement and strain in a vascular model. *Ultrason Imaging*. 1997;19:19–38.
17. Shapo BM, Crowe JR, Erkamp R, et al. Strain imaging of coronary arteries with intraluminal ultrasound: experiments on an inhomogeneous phantom. *Ultrason Imaging*. 1996;18:173–191.
18. de Korte CL, van der Steen AFW, Céspedes EI, et al. Intravascular ultrasound elastography of human arteries: initial experience in vitro. *Ultrasound Med Biol*. 1998;24:401–408.
19. Céspedes EI, de Korte CL, van der Steen AFW. Echo decorrelation from displacement gradients in elasticity and velocity estimation. *IEEE Transactions on Ultrasound, Ferroelectrics and Frequency Control*. 1999;46:791–801.
20. Dobrin PB. Mechanical properties of arteries. *Physiol Rev*. 1978;58:397–460.
21. Armitage P. *Statistical Methods in Medical Research*. Oxford, UK: Blackwell Scientific Publications; 1973.
22. Brezinski ME, Tearney GJ, Weissman NJ, et al. Assessing atherosclerotic plaque morphology: comparison of optical coherence tomography and high frequency ultrasound. *Heart*. 1997;77:397–403.
23. Römer TJ, Brennan JF III, Fitzmaurice M, et al. Histopathology of human coronary atherosclerosis by quantifying its chemical composition with Raman spectroscopy. *Circulation*. 1998;97:878–885.
24. de Korte CL, Woutman HA, van der Steen AFW, et al. IVUS elastography: a potential identifier of vulnerable atherosclerotic plaque. In: *IEEE Ultrasonics Symposium*. Sendai, Japan; 1998:1729–1732.
25. Céspedes EI, de Korte CL, van der Steen AFW. Intraluminal ultrasonic palpation: assessment of local and cross-sectional tissue stiffness. *Ultrasound Med Biol*. 2000;26:385–396.
26. Lee RT, Richardson G, Loree HM, et al. Prediction of mechanical properties of human atherosclerotic tissue by high-frequency intravascular ultrasound imaging. *Arterioscler Thromb*. 1992;12:1–5.
27. Lundberg B. Chemical composition and physical state of lipid deposits in atherosclerosis. *Atherosclerosis*. 1985;56:93–110.
28. van der Steen AFW, Cuypers MHM, Thijssen JM, et al. Influence of histochemical preparation on acoustical parameters of liver tissue, a 5 MHz study. *Ultrasound Med Biol*. 1991;17:879–891.
29. Gow BS, Hadfield CD. The elasticity of canine and human coronary arteries with reference to post-mortem changes. *Circ Res*. 1979;45:588–594.

## Characterization of Plaque Components With Intravascular Ultrasound Elastography in Human Femoral and Coronary Arteries In Vitro

Chris L. de Korte, Gerard Pasterkamp, Anton F. W. van der Steen, Hein A. Woutman and Nicolaas Bom

*Circulation*. 2000;102:617-623

doi: 10.1161/01.CIR.102.6.617

*Circulation* is published by the American Heart Association, 7272 Greenville Avenue, Dallas, TX 75231

Copyright © 2000 American Heart Association, Inc. All rights reserved.

Print ISSN: 0009-7322. Online ISSN: 1524-4539

The online version of this article, along with updated information and services, is located on the World Wide Web at:

<http://circ.ahajournals.org/content/102/6/617>

**Permissions:** Requests for permissions to reproduce figures, tables, or portions of articles originally published in *Circulation* can be obtained via RightsLink, a service of the Copyright Clearance Center, not the Editorial Office. Once the online version of the published article for which permission is being requested is located, click Request Permissions in the middle column of the Web page under Services. Further information about this process is available in the [Permissions and Rights Question and Answer](#) document.

**Reprints:** Information about reprints can be found online at:  
<http://www.lww.com/reprints>

**Subscriptions:** Information about subscribing to *Circulation* is online at:  
<http://circ.ahajournals.org/subscriptions/>